

Transient Stability Enhancement in Microgrids: Critical Clearing Time Assessment for Sequential Symmetrical and Asymmetrical Faults with PSS-SVC Coordination

Siradj Younes^{1*} , Sid Ahmed Tadjer² , Fathia Chekired³ .

^{1,2}Electrification of Industrial Enterprises Laboratory, University of Boumerdes, Boumerdes, Algeria.

³MUnité de Développement des Équipements Solaires, UDES, Centre de Développement des Energies Renouvelables, CDER, Bou Ismail, Tipaza, Algeria.

E-mail: ¹y.siradj@univ-boumerdes.dz, ²s.tadjer@univ-boumerdes.dz, ³f.chekired@cder.dz.

ARTICLE INFO.

Article history:

Received 13 Sep 2024

Received in revised form 15 Sep 2024

Accepted 22 Feb 2025

Available online 4 Mar 2025

KEYWORDS

Sequential faults, Transient stability, CCT, PSS-SVC, PV-Wind.

ABSTRACT

The widespread integration of renewable energy sources, such as photovoltaic (PV) and wind power, poses significant challenges to power system stability. This study investigates the combined effect of a Power System Stabilizer (PSS) and a Static Var Compensator (SVC) in enhancing transient stability during sequential symmetrical and asymmetrical faults. A modified IEEE 9-bus system was used, with PV arrays connected to Buses 5 and 6 and a wind farm integrated at Bus 8. Simulations were conducted using ETAP 20.2, with Critical Clearing Time (CCT) calculated and frequency/voltage variations analyzed.

The results demonstrate that the coordinated use of PSS and SVC significantly improves system stability, increasing CCT values and damping critical oscillations. The system showed enhanced resilience to sequential faults, providing practical solutions for renewable energy integration challenges. The key conclusion is that PSS-SVC coordination effectively enhances the flexibility of power systems under high renewable energy penetration.

*Corresponding author.

DOI: <https://doi.org/10.51646/jsesd.v14i1.478>

This is an open access article under the CC BY-NC license ([http://Attribution-NonCommercial 4.0 \(CC BY-NC 4.0\)](http://Attribution-NonCommercial 4.0 (CC BY-NC 4.0))).



تعزير الإستقرار المنتقل في الشبكات الصغيرة: تقييم زمن الإزالة الحرج للأخطاء المتسلسلة المتماثلة وغير المتماثلة باستخدام تنسيق (PSS-SVC)

يونس سیراج، سيد احمد تاجر، شكير فتحيّة.

ملخص: يشكل الدمج الواسع لمصادر الطاقة المتجددة، مثل الطاقة الكهروضوئية وطاقة الرياح، تحديات كبيرة لاستقرار الأنظمة الكهربائية. في هذه الدراسة، تم تحليل تأثير الجمع بين مثبت استقرار النظام (PSS) ومُعوّض القدرة غير الفعالة الثابت (SVC) لتعزيز الاستقرار العابر أثناء الأعطال المتتالية المتناظرة وغير المتناظرة. تم استخدام نموذج معدل لنظام 9-IEEE-حافلة مع إضافة ألواح كهروضوئية في قضبان التوصيل 5 و6 ومزرعة رياح في قضيب التوصيل 8. تم إجراء المحاكاة باستخدام برنامج ETAP 20.2، مع حساب زمن إزالة الخطأ الحرج (CCT) وتحليل التغيرات في التردد والجهد.

أظهرت النتائج أن استخدام PSS و SVC معاً يحسن بشكل كبير من استقرار النظام، حيث أدى إلى زيادة قيم CCT وتخميند الاهتزازات الحرجة. كما لوحظ أن النظام أصبح أكثر قدرة على التعامل مع الأعطال المتتالية، مما يوفر حلاً عملياً لتحديات دمج الطاقة المتجددة. الاستنتاج الرئيسي هو أن التنسيق بين PSS و SVC يعزز بشكل فعال من مرونة الأنظمة الكهربائية في ظل وجود مصادر طاقة متجددة.

الكلمات المفتاحية - الأعطال المتتالية، الاستقرار العابر، PV-Wind, PSS-SVC, CCT.

1. INTRODUCTION

Renewable energy sources are a crucial substitute for the Algerian economy, which heavily depends on natural gas for more than 98% of its electricity generation [1]. Due to the rising population and the expanding industrial developments, there has been a substantial increase in the demand for electrical energy. On July 18, 2024, the Algerian society “Société nationale de l'électricité et du gaz” (SONELGAZ) documented a significant surge in power usage, reaching a record peak of 19135 megawatts [2].

Algeria's extensive in solar energy make it possible to fulfill the worldwide need for electrical energy by utilizing an area of 254 km × 254 km in the country's southeastern region, according to the German researcher Nadine May [3]. Algeria has, turned to exploiting solar energy by integrating it into the national electrical grid. Similarly, wind energy has also been incorporated, exemplified by a wind farm in the Adrar province. Algeria has initiated the national renewable energy program to generate 22000 megawatts of solar energy by 2030. [4]

Ensuring the safe and reliable operation of the electrical grid relies heavily on the stability of the electrical system [5,6]. An overarching challenge in the electrical energy business is effectively managing the equilibrium between production and demand [7], Algeria has vital industries that rely on uninterrupted electricity, such as research, education, and healthcare.

The sporadic nature of renewable energy resources poses a hindrance to their widespread utilization in power generation. This renders them susceptible to grid fluctuations and voltage instability, be it caused by abrupt declines or unforeseen surges in voltage. Therefore, integrating the conventional electrical grid and renewable energies is feasible if there is continuous monitoring of the stability condition. The ability of smart grids to integrate renewable energy, like wind and photovoltaic, into the public electricity grid sets them apart.

The main focus of the study conducted by Yanbo et al [8] was to examine the quality of energy generated from renewable sources and its integration into the network. The study revealed several key quality issues in the integrated network, including voltage dips, interruptions, overvoltages, and voltage instability [11].

Several studies have been carried out to investigate these problems and their influence on the stability of networks that incorporate renewable energy sources, such as smart grids. According to a network stability analysis conducted by Maizana et al [9], it was shown that if the capacity of

sun cells does not surpass or match the system's load capacity, depending entirely on solar cells could hurt the stability of voltage and frequency in the system.

In the same vein, the research presented by Liaqat et al [10] conducts a transient stability for multi-microgrids by integrating UPFC and renewable energy in various scenarios. It is now necessary to connect the system to stability control devices to survive any disruptions in the grid [11,12]. Therefore, it is of utmost importance to reduce electrical disturbances, as the primary goals of employing FACTS (Flexible Alternating Current Transmission Systems) devices are control, network management, and quality enhancement [13]. Absar et al [14] describes a study to enhance the energy quality in a hybrid system that combines solar and wind energy. This was achieved through the integration an SVC device in the dynamic regime.

The work presented in the present study provides an in-depth analysis of the stability of systems integrated with renewable energy sources. We have adopted an approach based on sequential fault analysis, offering a deeper insight into system response under more complex conditions compared to studies limited to single faults.

Additionally, various scenarios have been examined involving different weather conditions during the supply of renewable energy sources, allowing for a more precise understanding of how these sources are distributed within the network and their impact on stability. Furthermore, SVC and PSS technologies have been integrated into analysis, enhancing the system's dynamic response and reducing the risk of instability, the Critical Clearing Time (CCT) as a key analytical tool, making results more accurate. To achieve this, we rely on the Newton-Raphson analysis technique using ETAP (Electrical Transient Analyzer Program) [15].

2. METHODOLOGY

We obtained the CCT values using a simulation-based approach. In each case, a fault introduced in the affected bus at $t = 1$ s and then cleared after a duration T_d . To determine the CCT, we conducted successive experiments, gradually increasing T_d by 1 millisecond in each trial until we identified the critical threshold beyond which the system transitioned from stability to instability. Where :

- **Fault Duration (T_d) :**

- o The actual time interval during which the fault persists before being cleared.
- o Measured from the moment the fault occurs until its removal.
- o Varies across simulation experiments, as it is gradually increased to assess system stability.
- o In this study, T_d was incremented by 1 millisecond per experiment to determine the CCT.

- **Critical Clearing Time (CCT) :**

- o The maximum allowable fault duration that the system can withstand without losing stability.
- o If the fault is cleared at or before CCT, the system remains stable.
- o If the fault duration T_d exceeds CCT, the system becomes unstable, leading to loss of synchronization or system collapse.

Thus :

- **If $T_d \leq CCT \rightarrow$ The system remains stable.**
- **If $T_d > CCT \rightarrow$ The system becomes unstable.**

To evaluate the stability of the system, in the transient phase, monitoring the generators' rotor angle behaviour is done. The purpose is to assess whether the system remains stable after a fault occurs. If the angular velocities of all three generators converge or approach a single synchronized angular velocity, then the system is stable. However, that the angular velocity of at least one of the three generators diverges, this indicates that the system is unstable.

2.1. Description and System configuration

For this investigation, ETAP 20.2 is used for simulation. The Newton-Raphson method [15] is utilized to do a transient analysis of the system. ETAP is an essential software tool for analysing systems' dynamic performance under different operating situations. ETAP enables transient system analysis and supports load flow analysis, motor starting analysis, and various other research on electrical systems [16].

The focus of the present study is the transient stability of a modified IEEE 9-bus system model. We have put four (4) PV array on Bus 6. Bus 5 was connected to three (3) PV array, while Bus 8 was tied to a three (3) of wind turbine generators, Figure 1.

Electrical networks commonly have problems, particularly defects in transmission lines and buses, resulting in grid disruptions. Thus, in the study 1 of our investigation, we deliberately caused individual failures at all significant nodes in the network and subsequently determined the Critical Clearing Time (CCT) for each occurrence.

In the study 2, we introduced two consecutive faults in each case. Based on the results from the first study, we determined the time interval between the faults, which corresponds to the time required for the system to achieve a new steady state after the first fault, four scenarios within this study tested transient stability in terms of sequential faults based on connectivity.

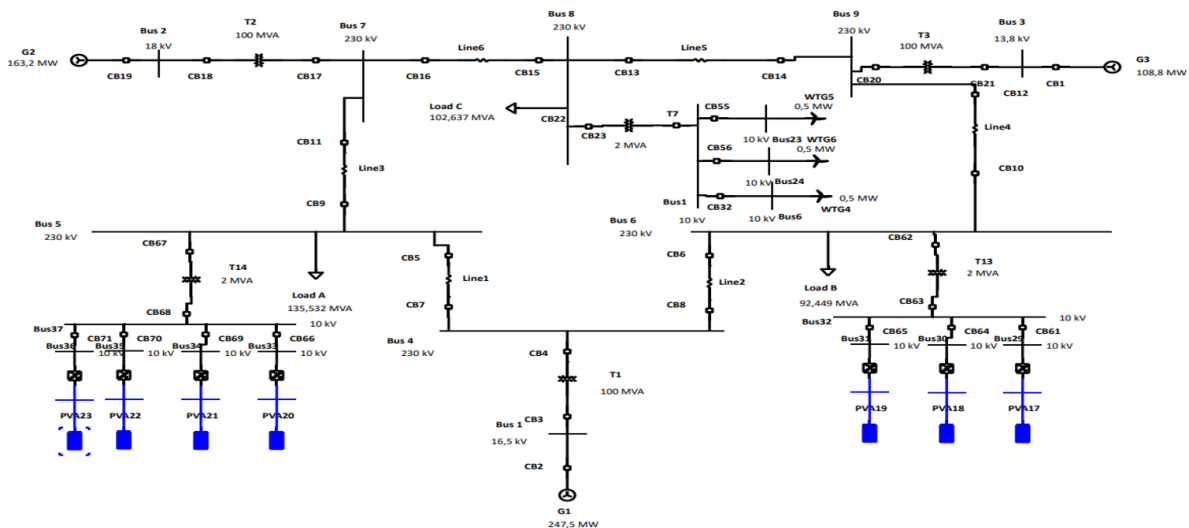


Figure 1. Modified IEEE 9-bus System Model in ETAP.

Table 1. Different Scenarios.

Study1: Symmetrical and unsymmetrical single fault		
Study 2: Sequential faults based on connectivity		
scenario	PV Array	Wind
Sc1	out	Out
Sc2	in	In
Sc3	out	In
Sc4	in	Out
Study3: Sequential faults based on percentage of PV and Wind		
scenario	PV Array	Wind
Sc1	80%	50%
Sc2	40%	25%
Sc3	20%	5%
Study4: Impact of svc and PSS		

While the third study 3 focused on examining transient stability in terms of sequential faults based on the percentage of PV and wind integration.

In the study 4, we integrated the SVC and the PSS and studied their effects on transient stability enhancement.

2.1.1. Synchronous Generators

The dataset contains information about synchronous generators, including bus ID, voltage levels, operation type, and power generation in megawatts. These data are essential for analyzing generator performance and operational behavior, as indicated in table 2.

Table 2. Dynamic data of the generators.

ID	Generation Bus		Generation MW
	kV	Type	
Bus 1	16,500	Swing	247.500
Bus 2	18,000	Voltage Control	163,200
Bus 3	13,800	Voltage Control	108.800

2.1.2. PV Solar

Photovoltaic energy has become a prominent renewable energy source nowadays due to its versatility, technological simplicity, recent cost reductions, and minimal maintenance needs. Photovoltaic panels consist mainly of silicon, which functions as a semiconductor. Photovoltaic cells produce electrical energy by using the photovoltaic effect. [20]

The integration of solar energy into traditional electrical grids has become one of the major challenges in the field of electrical power.

Photovoltaic panels are employed in this system, as they have the ability to transform photons from light into electrical energy due to their semiconductor properties. This design has a series connection of 59 PV panels and a parallel connection of 154 PV panels. Every photovoltaic (PV) array has a power rating of 1 megawatt (MW).

The technical specifications of photovoltaic panels are outlined in the table 3.

Table 3. The specifications of the module PV PHOTWATT Multi-crystalline PW6-110

Specifications	Values
Maximum power (Pm)	110W
Open-Circuit Voltage (Voc)	21.69V
Short-Circuit Current (Isc)	6.93A
Maximum power voltage (Vmpp)	17.18V
Maximum power current (Impp)	6.42A
Open-Circuit Voltage temperature coefficient (kv)	-0,3641 % / K
Short-Circuit Current temperature coefficient (ki)	0,0302 % / K

2.1.3. WIND

Wind turbines produce wind energy, which is categorized as an electromechanical energy source. It is a widely embraced substitute for fossil fuels, serving as a sustainable energy source. Equation (1) represents the amount of wind power that can be extracted:

$$P = \frac{1}{2} \times \rho \times A \times V^3 \times C_p \tag{1}$$

$$A = \pi r^2$$

ρ : Density of air.

A: Swept area of turbine blades.

V : Wind speed.

C_p : Power coefficient.

r : Radius of the blades.

The wind turbine has a capacity of 0.5 MW. The nominal power factor is 0.85, the nominal voltage of the wind turbine is 10 kV, the nominal efficiency is 0.95, and the nominal wind speed is 10 m/s. Table 4. represents electrical parameters of the used wind turbine.

Table 4. Specifications of the wind turbine.

Parameters	Values
Rotor diameter D	60m
Number of pales n	3
Generator	AC
Speed of Start-up, Vd	4m/s
Nominal speed, Vn	10m/s
Stop speed; VA	25m/s

2.1.4. Line

The dataset provides details about transmission lines, such as length, resistance, reactance, and admittance. These values play a crucial role in power flow analysis and assessing the stability of electrical networks, as indicated in table 5.

Table 5. Line data.

ID	Length (ft)	R	X	Y
Line1	1000,0	5,290000	44,965400	0,0003327
Line2	1000,0	8,993000	48,668000	0,0002987
Line3	1000,0	16,928000	85,169000	0,0005785
Line4	1000,0	20,631000	89,930000	0,0006767
Line5	1000,0	6,295100	53,323200	0,0003951
Line6	1000,0	4,496500	38,088000	0,0002817

2.1.5. Static VAR Compensator SVC

The SVC is a controllable power electronics device designed to stabilize voltage in steady-state and transient conditions. Its primary function is to rapidly regulate voltage through the injection or absorption of reactive power into the bus where the reactive power demand of the load is installed [17].

Figure 2, illustrates the characteristic curve of a Static VAR Compensator (SVC), depicting the relationship between terminal voltage (V_T) and the output current (I_{SVC}). The curve demonstrates the voltage regulation behavior of the SVC in both capacitive and inductive modes. In this simulation, a reactive compensation capacity of 200 Mvar is configured in capacitive mode and 200 Mvar in inductive mode for the SVC.

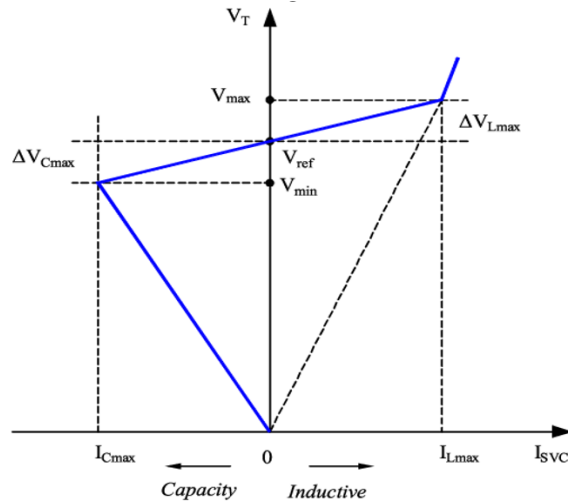


Figure 2. Characteristic curve of SVC [17].

2.1.6. Power System Stabilizer PSS

The PSS is employed to enhance the stability of the electrical system by reducing the amplitude of rotor oscillations in synchronous generators. These oscillations may arise due to slight fluctuations in the load or voltage. We employed the IEEE Type 1 PSS (PSS1A) for our simulation, as depicted in Figure 3.

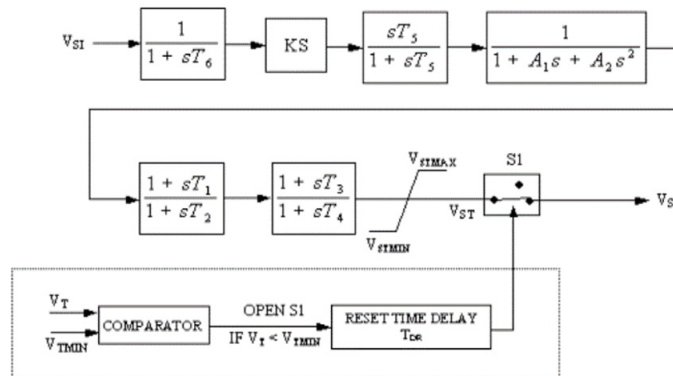


Figure 3. IEEE Type 1 PSS (PSS1A) [15].

2.1.7. Transformation

Table 6, presents the key electrical parameters of transformers, such as transformer ID, phase type, power rating (MVA), primary and secondary voltage levels (kV), impedance values (%Z1, X1/R1, %Z), and phase angle. These parameters are essential for analyzing transformer performance, voltage regulation, and overall power system stability.

Table 6. The Dataset of Transformer Parameters.

ID	Phase	MVA	Prim. kV	Sec. kV	% Z1	X1/R1	% Z	Angle
T1	3-Phase	100	230	16,5	5,76	1000	5,7600	0,00
T2	3-Phase	100	18	230	6,25	1000	6,2500	0,00
T3	3-Phase	100	13,8	230	5,86	1000	5,8600	0,00
T7	3-Phase	2,00	10	230	10,00	7,10	10,0000	0,00
T13	3-Phase	2,00	10	230	10,00	7,10	10,0000	0,00
T14	3-Phase	2,00	10	230	10,00	7,10	10,0000	0,00

2.2. Equations

The positional relative between the axis of the rotor and the axis of the magnetic field remains constant during the normal operation of a generator, unaffected by any disruptions. The power angle refers to the angle formed between these two axes.

The rotor may experience relative motion when a disturbance occurs, causing it to either slow down or accelerate up about the synchronously rotating magnetic flux. The swing equation describes this relative motion[26]:

$$M \frac{d^2 \delta}{dt^2} = P_a = P_m - P_e \tag{2}$$

$$M = \frac{2H}{\omega_s} \tag{3}$$

P_a : Accelerating power.

P_m : Mechanical power.

P_e : Electrical power output.

ω_s : Synchronous angular velocity of the rotor.

δ : Rotor angle.

M : Inertia constant coefficient.

H : Inertia constant of the machine.

2.3. Equal-area criterion

The equal-area criteria is an analytical technique for investigating transient stability in the single-machine infinite-bus system (SMIB). This approach, employing the Swing Equation (2), aids in calculating the critical clearing angle (4), the critical clearing time (5), and the overall stability condition of the system.

$$\delta_{cr} = \cos^{-1} [(\pi - 2\delta_0) \sin \delta_0 - \cos \delta_0] \tag{4}$$

$$t_{cr} = \sqrt{\frac{4H(\delta_{cr} - \delta_0)}{\omega_s}} \tag{5}$$

$$|area A1| = |area A2| \tag{6}$$

δ_{cr} : Critical clearing angle.

δ_0 : Initial rotor angle.

ω_s : synchronous angular velocity.

The areas A1 and A2 correspond to the kinetic energy accumulated in the rotor as it speeds up and slows down, respectively. The acceleration area (Positive area) must be equivalent to the deceleration area (Negative area) to ensure system stability (6). The criteria mentioned are commonly called the equal area criterion, as depicted in Figure 4:

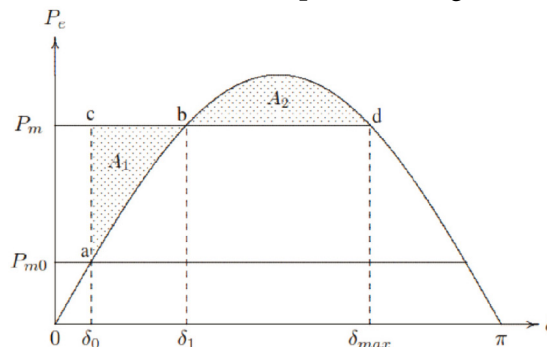


Figure 4. Equal-area criterion of sudden change of load. [18].

3. STATISTICAL AND DATA ERRORS

The initial load flow analysis was performed using the Newton-Raphson method due to its numerical accuracy and efficiency in load flow calculations. The maximum number of iterations was set to 9999 to ensure convergence, with a solution precision of 0.000001, providing a high level of accuracy in computations.

Although the Newton-Raphson method is widely used for its ability to handle nonlinear networks, it may experience convergence issues in certain cases, particularly when initial values are inappropriate or when dealing with highly unstable systems. Additionally, numerical errors arising from the approximation of differential equations within ETAP software may influence the computed values of the Critical Clearing Time (CCT).

To verify the consistency of results and minimize the impact of potential numerical errors, multiple simulations were performed under the same settings. These tests demonstrated that the variations caused by numerical errors were not significant enough to affect the study's main conclusions.

4. RESULTS AND DISCUSSIONS

Various fault scenarios have been done in order to analyze power system behavior under different conditions. Study 1 examines symmetrical and unsymmetrical single faults, Study 2 investigates sequential faults based on connectivity, Study 3 explores sequential faults by varying the percentage of PV and wind penetration, evaluating their impact on grid stability. Study 4 assesses the influence of Static VAR Compensator (SVC) and Power System Stabilizer (PSS) in improving system performance under different operating conditions.

4.1. Study N°1

This study aims to determine the Critical Clearing Time (CCT) for single symmetrical and unsymmetrical faults in a microgrid and assess their impact on transient stability. The results show that the system remains stable for a fault duration (T_d) of 0.429 seconds, but loses stability at 0.430 seconds, confirming that the CCT for this case is 0.429 seconds.

Our findings confirm that 3-phase symmetrical faults (3PH) have the most severe impact on stability, the CCT values for line-to-line (LL) and line-to-line-to-ground (LLG) faults are generally higher, indicating that these faults allow a longer tolerance before instability occurs.

Han et al [21] and Seyedi et al [22] suggest that CCT the level of renewable integration.

The shorter CCT for bus 6 faults in our study is consistent with research showing that faults closer to critical system components (e.g., generators) lead to faster loss of stability.

Understanding the CCT for different fault types is crucial for designing protective schemes that ensure system stability.

Figure 5. illustrates the rotor angle (a), frequency (b), and voltage (c) responses of the system following a temporary 3-phase fault at bus 6 with a fault duration (T_d) of 0.429 seconds, demonstrating the system's ability to maintain stability under transient conditions:

a) Rotor Angle:

The graph illustrates the rotor angle. The system remains stable as the rotor angles of all generators converge to a synchronized state after the fault is cleared at $T_d = 0.429s$. This indicates that the system can maintain synchronism under transient conditions.

b) Frequency:

The frequency response of the system is depicted, showing that the system frequency stabilizes within acceptable limits after the fault is cleared. This demonstrates the system's ability to maintain frequency stability despite the temporary disturbance.

c) Voltage:

The voltage profile at bus 6 is illustrated, indicating that the voltage recovers to its nominal value after the fault is cleared. This confirms that the system maintains voltage stability under the given fault conditions.

Figure 6. illustrates the rotor angle (a), frequency (b), and voltage (c) responses of the system following a temporary 3-phase fault at bus 6 with a fault duration (T_d) of 0.430 seconds, demonstrating the system's transition from stability to instability as the fault duration exceeds the critical clearing time (CCT):

b) Rotor Angle:

The graph shows the rotor angle. The system becomes unstable as the rotor angles of the generators diverge after the fault is cleared at $T_d = 0.430s$, indicating a loss of synchronism.

c) Frequency:

The frequency response of the system is shown, indicating that the system frequency deviates significantly from the nominal value after the fault is cleared. This demonstrates the system's inability to maintain frequency stability under transient conditions.

d) Voltage:

The voltage profile at bus 6 is depicted, showing that the voltage fails to recover to its nominal value after the fault is cleared. This indicates a loss of voltage stability, further confirming the system's instability.

The data presented in Table.7 shows a CCT Value for each fault on the Microgrid buses 4, 6, 7, 8, and 9.

Table 7. The CCT values with a single fault.

Faulted bus	CCT (3ph Fault) (ms)	CCT (LL Fault) (ms)	CCT (LLG Fault) (ms)
4	312	659	495
5	382	905	459
6	429	930	512
7	221	334	304
8	309	868	528
9	253	394	314

4.2. Study N°2

This study examines the effect of sequential faults on the transient stability of the microgrid. Two distinct fault sequences were analyzed:

- LL fault followed by a 3PH fault
- LLG fault followed by a 3PH fault

The first fault occurs at $t = 1s$, lasting 0.3 seconds, and is cleared at $t = 1.3s$. Immediately after, a second 3PH fault is introduced at $t = 1.4s$ and persists until the system reaches instability, determining the CCT for each case.

The study explored different renewable energy scenarios, (Table 8) considering the connection or disconnection of wind and photovoltaic (PV) energy sources. The results reveal that connectivity status significantly influences CCT during sequential faults:

- The system exhibited greater sensitivity and susceptibility to disturbances when connected to renewable energy sources.
- CCT values were notably lower in the presence of photovoltaic energy, indicating a higher risk of instability.

- The integration of wind energy also affected stability, but to a lesser extent than PV energy.

Table 8. The CCT values with sequential faults based on connectivity.

Faulted bus	Scenario 1		Scenario 2		Scenario 3		Scenario 4	
	CCT (LL-3Ph Faults) (ms)	CCT (LLG-3Ph Faults) (ms)	CCT (LL-3Ph Faults) (ms)	CCT (LLG-3Ph Faults) (ms)	CCT (LL-3Ph Faults) (ms)	CCT (LLG-3Ph Faults) (ms)	CCT (LL-3Ph Faults) (ms)	CCT (LLG-3Ph Faults) (ms)
4	271	259	266	253	269	257	264	255
5	397	389	388	384	394	392	390	388
6	472	452	458	449	468	465	461	461
7	146	141	140	138	145	144	140	138
8	305	296	297	293	302	300	297	296
9	252	243	235	231	237	234	233	231

Our findings align with some previous studies, such as [23], which indicated that a higher penetration of renewable energy reduces system inertia, making microgrids more vulnerable to instability during faults. However, this study did not consider the impact of sequential faults, as it focused solely on single faults, making its conclusions insufficient for describing the behavior of modern systems with high renewable energy integration.

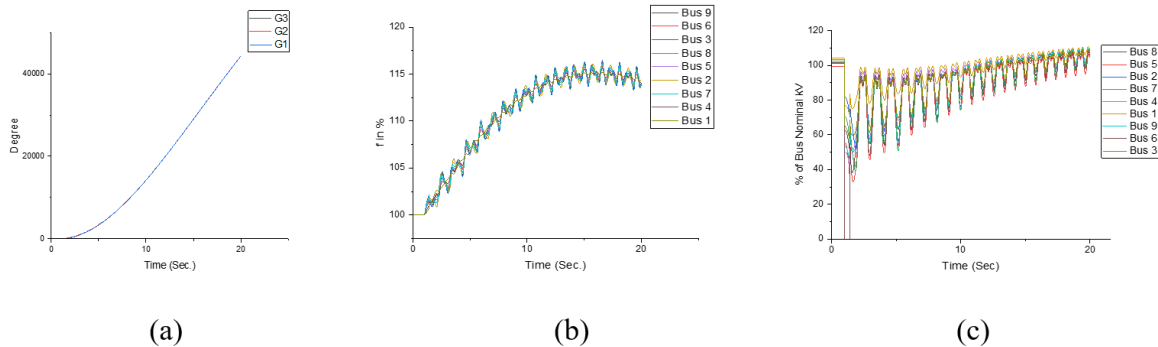


Figure 5. Rotor angle (a), frequency (b), and voltage (c) for a temporary 3-ph fault at bus 6 with $T_d = 0.429s$ (Stable System).

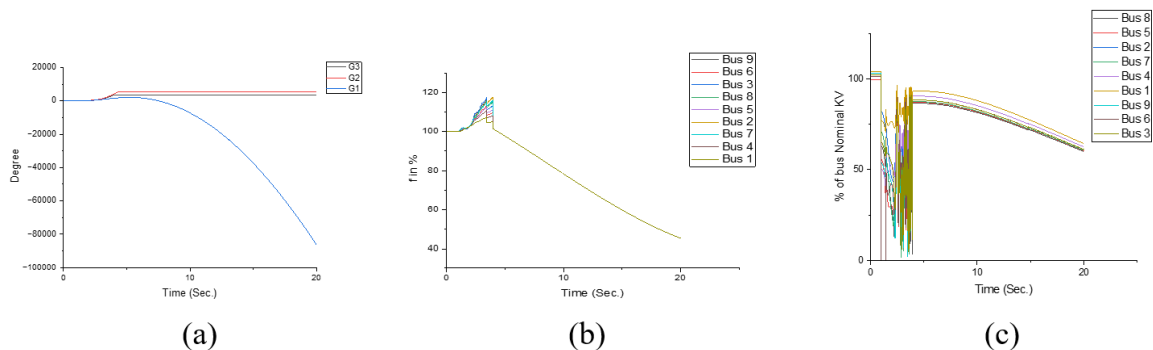


Figure 6. Rotor angle (a), frequency (b), and voltage (c) for a temporary 3-ph fault at bus 6 with $T_d = 0.430s$ (Unstable System).

4.3. Study N°3

This study aims to analyze the impact of fluctuations in photovoltaic (PV) and wind energy production on the stability of the power system during sequential faults. The results indicate that these fluctuations significantly affect the Critical Clearing Time (CCT), reducing the system's ability to withstand faults before losing stability. Table 9 shows that sudden drops in renewable energy production lead to lower CCT values, making the system more susceptible to instability during sequential faults.

Many have focused on the impact of the penetration level of renewable energy into the grid but have not thoroughly examined the dynamic effects of actual production fluctuations. For example:

Some studies [27,28] have focused on determining the maximum allowable percentage of renewable energy before the system loses stability but did not consider momentary weather-related variations such as cloud cover and sudden drops in wind speed.

This study confirms that fluctuations in renewable energy reduce the system's ability to withstand sequential faults.

Table 9. The CCT values for sequential faults based on the percentage of PV and wind.

Faulted bus	scenario 1		scenario 2		scenario 3	
	CCT LL-3Ph Faults (ms)	CCT LLG-3Ph Faults (ms)	CCT LL-3Ph Faults (ms)	CCT LLG-3Ph Faults (ms)	CCT LL-3Ph Faults (ms)	CCT LLG-3Ph Faults (ms)
4	268	253	270	254	270	257
5	391	379	395	382	396	382
6	464	444	467	445	469	449
7	144	140	145	140	146	137
8	301	286	303	289	303	290
9	236	230	237	230	247	233

4.4. Study N°4

This study explores how the integration of Static VAR Compensator (SVC) and Power System Stabilizer (PSS) affects the transient stability of the system under sequential symmetric and asymmetric faults. The system is tested with full photovoltaic (PV) and wind energy integration to assess its resilience to disturbances.

The results indicate that the joint integration of SVC and PSS significantly enhances system stability by:

- Reducing oscillations in rotor angle and frequency after sequential faults.
 - Extending the Critical Clearing Time (CCT), allowing the system to withstand faults for a longer duration before instability occurs.
 - Mitigating voltage fluctuations, ensuring a more stable recovery to nominal voltage after faults.
- The findings confirm that optimal SVC placement is crucial for maximizing its impact on voltage stability, as demonstrated by our selection of Bus 7, which exhibited the most significant voltage fluctuations.

Previous studies mentioned in [19] have analyzed FACTS devices like SVC in power system stability; however, many focus on single-fault events rather than sequential faults with high renewable penetration.

- SVC combined with PSS provides better overall stability, especially in managing frequency deviations and damping oscillations.
- Research [17] has emphasized the importance of SVC placement for maximum effectiveness, aligning with our finding that installing SVC at the most voltage-sensitive bus (Bus 7) yields superior results.
- Previous studies [29,30] suggest that PSS alone is effective for damping oscillations but does not significantly enhance voltage stability. Our results reinforce that coordinating SVC with PSS offers a more comprehensive solution.

The results underscore the importance of coordinated control strategies for power system stability in renewable-integrated networks. The key takeaways are:

1. Combining SVC and PSS enhances stability across multiple aspects (voltage, frequency, and rotor angle synchronization).
2. Optimal placement of SVC is necessary to achieve maximum voltage stability improvement.

Figures 7. (a) and Figure 8. (a) depict the voltage angle versus time diagrams for successive LL-3PH and LLG-3PH faults. The diagrams are shown under three different conditions: when both SVC and PSS are present, when only SVC is present, and when neither SVC nor PSS are present. The voltage angle diagram exhibits pronounced oscillations without both SVC and PSS. For Figure 7. (b), (c) and Figure 8. (b), (c), which show the voltage versus time diagrams for sequential LL-3PH and LLG-3PH faults under the following conditions: the presence of both SVC and PSS, and the absence of both SVC and PSS, it can be observed that the joint integration of PSS and SVC leads to improved stability by enhancing damping. This enhancement can reduce oscillations and fluctuations that contribute to instability.

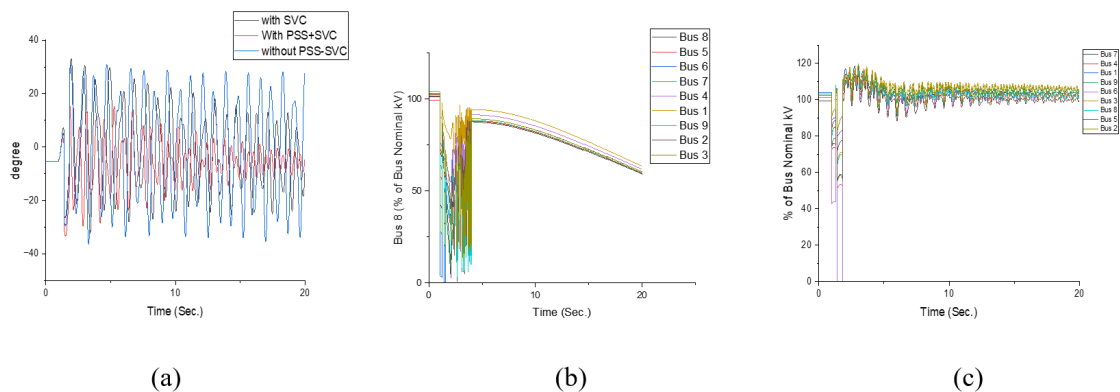


Figure 7. Sequential LL-3Ph fault at bus 6 with $T_d = 0.506s$: Voltage angle (a), voltage without svc+pss (b), voltage with svc+pss (c).

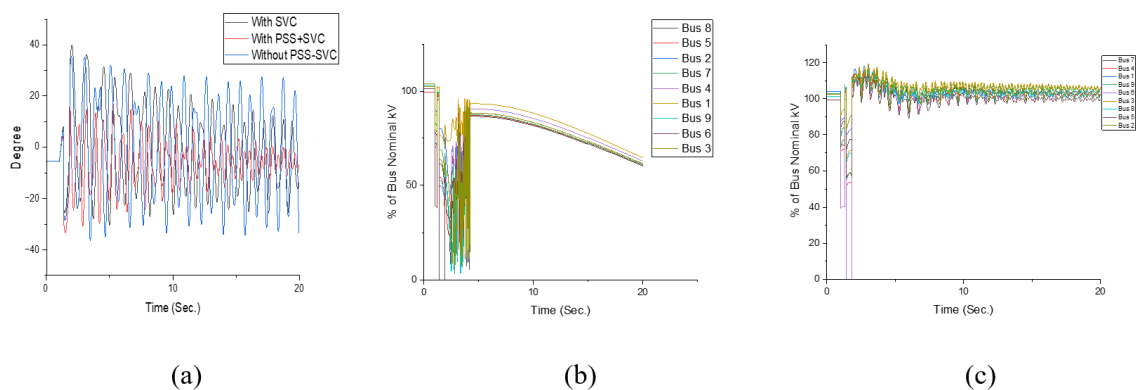


Figure 8. Sequential LLG-3Ph fault at bus 6 with $T_d = 0.498s$: Voltage angle (a), voltage without svc+pss (b), voltage with svc+pss (c).

The CCT results in Table 10 demonstrate the effect of the SVC and PSS in mitigating the negative impacts of faults on the network by improving voltage response. This has contributed to enhancing the system’s capability to handle faults over more extended periods, thereby increasing the CCT during transient conditions with sequential faults, compared to the absence of the SVC and PSS, as shown in Table 10.

Table 10. The CCT values with a sequential fault with SVC+PSS.

Faulted bus	CCT (LL-3ph Faults) (ms)	CCT (LLG-3ph Faults) (ms)
4	275	261
5	404	393
6	463	456
7	158	139
8	309	307
9	238	233

The following Figure 9. summarizes a comparison of the CCT values for sequential faults LL-3PH and LLG-3PH across buses 4, 5,6, 7, 8, and 9, both with and without SVC and PSS.

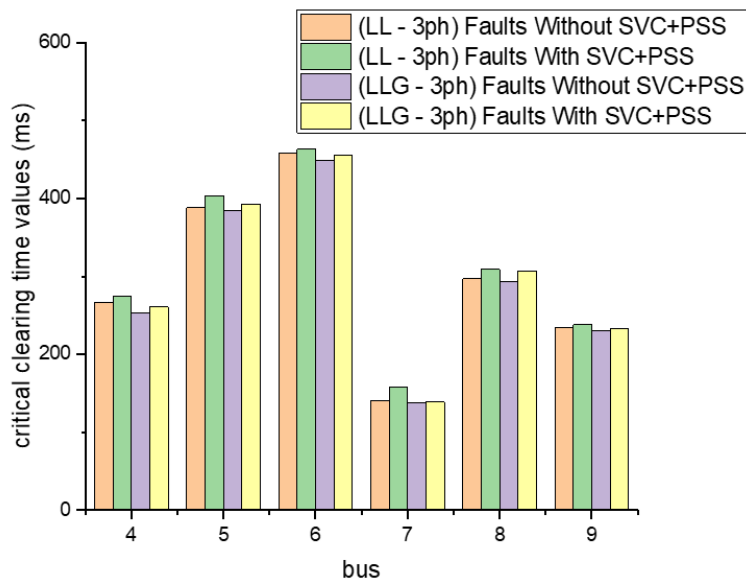


Figure 9. Comparing of the CCT values.

5. CONCLUSION

In this study, we analyzed the impacts of photovoltaic (PV) and wind energy integration on transient stability, with a focus on the effectiveness of SVC and PSS in mitigating sequential symmetrical and asymmetrical faults. For this purpose, four different scenarios were examined, considering variations in renewable energy connection and supply conditions.

The findings highlight that among single faults, a three-phase (3Ph) fault poses the highest risk to system stability. However, a detailed analysis of voltage behavior and rotor angle reveals that the sequential LLG-3Ph fault has a more significant impact on microgrid stability. This conclusion is supported by the measured Critical Clearing Time (CCT) values, which indicate a shorter stability threshold for LLG-3Ph faults compared to LL-3Ph faults. The reduced CCT values demonstrate a

faster deterioration of system stability, emphasizing the severity of sequential faults.

Additionally, the study reveals that fluctuations in the connection status and power production of wind and PV energy substantially reduce CCT values, thereby exacerbating system instability during sequential fault conditions. The integration of SVC and PSS has shown a considerable positive effect on enhancing transient stability in hybrid microgrids. These devices improve voltage stability, provide rapid fault support, and mitigate the mechanical and electrical oscillations caused by successive faults, ultimately accelerating system recovery.

Despite the insights provided by this study, certain limitations exist. The simulations were based on a modified IEEE 9-bus model, which may not fully capture the complexities of large-scale power networks. Additionally, idealized operating conditions were assumed, neglecting factors such as demand fluctuations. The authors are currently working on real-time experimental studies at a hybrid power generation plant in GHARDAIA city located in the northern Algerian desert, these studies aim to enhance the accuracy and applicability of our findings while enabling a deeper investigation into the role of FACTS devices in improving power system stability.

Authors contribution: All authors have made a substantial, direct, and intellectual contribution to the work and approved it for publication.

Funding: This work did not receive any external funding.

Data Availability Statement: Data will be available upon request.

Conflicts of Interest: The authors declare that they have no conflict of interest.

REFERENCES

- [1] ATTAR, M. A., *ransitionet Sécurité Énergétique les Défis à L'horizon 2030, Revue Algérienne des Politiques Publiques, Vol 08 : nr 03, 2020.*
- [2] Sonelgaz : *Un Quatrième Nouveau Pic de consommation électrique enregistré Durant l'été 2024. Radio Algérienne n.d. <http://news.radioalgerie.dz/fr/node/48902> (accessed August 18, 2024).*
- [3] May, N. *Eco-balance of a solar electricity transmission from North Africa to Europe. Unpublished Diploma thesis, Technical University of Braunschweig, 2005.*
- [4] Nassima D. *Le gouvernement s'inscrit "pleinement" Dans la Stratégie de la transition énergétique à l'horizon 2035. APS 2024. <https://www.aps.dz/economie/166220-le-gouvernement-s-inscrit-pleinement-dans-la-strategie-de-la-transition-energetique-a-l-horizon-2035> (accessed August 18, 2024).*
- [5] L. Chilakapati, "Microgrid power quality enhancement with Adaptive Control Strategies: A literature survey," *PRZEGLĄD ELEKTROTECHNICZNY*, vol. 1, no. 3, pp. 115–119, Mar. 2024. <https://doi:10.15199/48.2024.03.21>.
- [6] T. RACHDI, "Performance enhancement of smart grid using an optimal placement of facts: Case of TCSC," *PRZEGLĄD ELEKTROTECHNICZNY*, vol. 1, no. 2, pp. 281–287, Feb. 2024. <https://doi:10.15199/48.2024.02.56>
- [7] L. Gan, P. Jiang, B. Lev, and X. Zhou, "Balancing of supply and demand of Renewable Energy Power System: A review and Bibliometric Analysis," *Sustainable Futures*, vol. 2, p. 100013, 2020. <https://doi:10.1016/j.sfr.2020.100013>
- [8] Che, Y., & Chen, J. *Research on design and control of microgrid system. Electrical Review ISSN, 33(2097), 83-86. 2012.*
- [9] D. Maizana, A. Rezky, S. Muthia Putri, H. Satria, and M. Mungkin, "Stability Analysis of Smart Grid Management System on campus building," *Indonesian Journal of Electrical Engineering and Computer Science*, vol. 30, no. 3, p. 1321, Jun. 2023. <https://doi:10.11591/ijeecs.v30.i3.pp1321-1330>
- [10] M. Liaqat, T. Alsuwian, A. A. Amin, M. Adnan, and A. Zulfiqar, "Transient stability enhancement in renewable energy integrated multi-microgrids: A comprehensive and

critical analysis,” *Measurement and Control*, vol. 57, no. 2, pp. 187–207, Sep. 2023. <https://doi:10.1177/00202940231196193>.

[11] H. Shayeghi, H. Aryanpour, M. Alilou, and A. Jalili, “Microgrid stability definition, analysis, and examples,” *Power Systems*, pp. 305–335, 2021. https://doi:10.1007/978-3-030-59750-4_13.

[12] S. Krishnamurthy and E. I. Ogunwole, “Microgrid system design, modeling, and simulation,” *Modeling and Control Dynamics in Microgrid Systems with Renewable Energy Resources*, pp. 345–376, 2024. <https://doi:10.1016/b978-0-323-90989-1.00009-9>

[13] R. Majumder, “Some aspects of stability in microgrids,” *IEEE Transactions on Power Systems*, vol. 28, no. 3, pp. 3243–3252, Aug. 2013. <https://doi:10.1109/tpwrs.2012.2234146>

[14] M. N. Absar, M. F. Islam, and A. Ahmed, “Power quality improvement of a proposed grid-connected hybrid system by load flow analysis using static VAR compensator,” *Heliyon*, vol. 9, no. 7, Jul. 2023. <https://doi:10.1016/j.heliyon.2023.e17915>

[15] “ETAP: Energy Management Solution: Electrical Digital Twin Platform,” Default, <https://www.etap.com/> (accessed Aug. 18, 2024).

[16] C. S. Kamble and Prof. R. Rewatkar, “Load-flow analysis of distribution systems using ETAP,” *ICSESD-2017, 2017*. <https://doi:10.24001/ijaems.icesd2017.95>

[17] N. M. Khoa, N. H. Hieu, and D. T. Viet, “A study of SVC’s impact simulation and analysis for distance protection relay on transmission lines,” *International Journal of Electrical and Computer Engineering (IJECE)*, vol. 7, no. 4, p. 1686, Aug. 2017. <https://doi:10.11591/ijece.v7i4.pp1686-1695>

[18] PARTON, John E. *A note on the equal-area stability criterion. Proceedings of the IEE-Part IV: Institution Monographs*, 1952, vol. 99, no 3, p. 187-193.

[19] Rebhaoui, A. *Emplacement Optimal Multi-objectif des Compensateurs Shunts dans les Réseaux Electriques de Distribution. Unpublished Diploma thesis, Ecole Nationale Polytechnique*, 2018.

[20] M. Al Hazza, H. Attia, and K. Hossin, “Solar photovoltaic power prediction using statistical approach-based analysis of variance,” *Solar Energy and Sustainable Development Journal*, vol. 13, no. 2, pp. 45–61, Jun. 2024. <https://doi:10.51646/jsesd.v13i2.181>

[21] Han, H., Luo, S., Chen, S., Yuan, L., Shi, G., Yang, Y., & Fei, L. *A transient stability enhancement framework based on rapid fault-type identification for virtual synchronous generators. International Journal of Electrical Power & Energy Systems*, 155, 109545. <https://doi.org/10.1016/j.ijepes.2023.109545> (2024)

[22] Seyedi, Y., Mahseredjian, J., & Karimi, H.. *Impact of fault impedance and duration on transient response of Hybrid AC/DC Microgrid. Electric Power Systems Research*, 197, 107298 (2021). <https://doi.org/10.1016/j.epsr.2021.107298>

[23] Hu, S., Yang, J., Wang, Y., Zhao, Y., & Chao, C. (2023). *Inertia and primary frequency response requirement assessment for high-penetration renewable power systems based on planning perspective. Sustainability*, 15(23), 16191. <https://doi.org/10.3390/su152316191>

[24] M. Aslan et al., “Performance enhancement of microgrid systems using backstepping control for grid side converter and MPPT optimization,” *Solar Energy and Sustainable Development Journal*, vol. 14, no. 1, pp. 19–41, Dec. 2024. doi:10.51646/jsesd.v14i1.367 [25]

[26] Z. SHUAI, *Transient Characteristics, Modelling and Stability Analysis of MICROGRID. S.l.: SPRINGER VERLAG, SINGAPOR*, 2021.

[27] Q. Wang, A. Xue, T. Bi, and Y. Zheng, “Impact of DFIG-based wind farm on transient stability of Single Machine Infinite Bus System,” *2013 IEEE PES Asia-Pacific Power and Energy Engineering Conference (APPEEC)*, pp. 1–5, Dec. 2013. doi:10.1109/appeec.2013.6837199

[28] T. K. Yudhantomo, L. M. Putranto, B. Sugiyantoro, and Tiyono, “Transient stability analysis in grid integrated solar farm,” *2019 5th International Conference on Science and Technology (ICST)*, pp. 1–6, Jul. 2019. doi:10.1109/icst47872.2019.9166213

- [29] S. R. Paital, P. K. Ray, and A. Mohanty, "Firefly-swarm optimized fuzzy adaptive PSS in power system for Transient Stability Enhancement," *2017 Progress in Electromagnetics Research Symposium - Fall (PIERS - FALL)*, pp. 1969–1976, Nov. 2017. doi:10.1109/piers-fall.2017.8293460
- [30] Z. Liu et al., "Research the influence of PSS on power system transient stability," *2022 IEEE International Conference on Artificial Intelligence and Computer Applications (ICAICA)*, pp. 134–138, Jun. 2022. doi:10.1109/icaica54878.2022.9844499
- .